Muscle contributions to centre of mass acceleration during turning gait in typically developing children: A simulation study.

Philippe C. Dixon[1], Karen Jansen[2], Ilse Jonkers[2], Julie Stebbins[3], Tim Theologis[3], Amy B. Zavatsky[1]

1. Department of Engineering Science, University of Oxford, Oxford, UK

2. Human Movement Biomechanics Research Group, Department of Kinesiology, KU Leuven, Belgium

3. Nuffield Orthopaedic Centre, Oxford University Hospitals NHS Trust, Oxford, UK

Keywords: turning gait, simulation, induced acceleration analysis, centre of mass, children

Article type: Original Article accepted for publication in *Journal of Biomechanics*

Word count: 3499

Abstract: 249

***Corresponding Author:**

Julie Stebbins

Tel.: +44 1865227609; fax: +44 1865227949.

E-mail address: julie.stebbins@ouh.nhs.uk

Abstract

Turning while walking requires substantial joint kinematic and kinetic adaptations compared to straight walking in order to redirect the body centre of mass (COM) towards the new walking direction. The role of muscles and external forces in controlling and redirecting the COM during turning remains unclear. The aim of this study was to compare the contributors to COM medio-lateral acceleration during 90° pre-planned turns about the inside limb (spin) and straight walking in typically developing children. Simulations of straight walking and turning gait based on experimental motion data were implemented in OpenSim. The contributors to COM global medio-lateral acceleration during the approach (outside limb) and turn (inside limb) stance phase were quantified via an induced acceleration analysis. Changes in medio-lateral COM acceleration occurred during both turning phases, compared to straight walking ($p < 0.001$). During the approach, outside limb plantarflexors (soleus and medial gastrocnemius) contribution to lateral (away from the turn side) COM acceleration was reduced ($p < 0.001$), whereas during the turn, inside limb plantarflexors (soleus and gastrocnemii) contribution to lateral acceleration (towards the turn side) increased ($p \leq 0.013$) and abductor (gluteus medius and minimus) contribution medially decreased ($p < 0.001$), compared to straight walking, together helping accelerate the COM towards the new walking direction. Knowledge of the changes in muscle contributions required to modulate the COM position during turning improves our understanding of the control mechanisms of gait and may be used clinically to guide the management of gait disorders in populations with restricted gait ability.

1. Introduction

The ability to turn while walking is an important feature of human locomotion accounting for 20–50% of all daily steps (Glaister et al., 2007; Sedgman et al., 1994). The majority of turns rotate the body between 76 and 120° (Sedgman et al., 1994), possibly leading many investigators to focus on 90° turns (Desloovere et al., 2010; Glaister et al., 2008; Grasso et al., 1998; Strike & Taylor, 2009; Taylor et al., 2005; Xu et al., 2004).

Turning is achieved via controlled movement of the body centre of mass (COM) towards the new walking direction (Courtine & Schieppati, 2003a; Patla et al., 1991). Although different turning strategies are described in the literature, in our investigation of pre-planned 90° turns, the spin strategy, in which the body rotates about the ipsilateral (inside) limb, with respect to the turning direction, was preferred by typically-developing (TD) children (Dixon et al., 2013). The spin turn develops over three phases (Glaister et al., 2008). During the approach phase, the contralateral (outside) limb, initiates the turn. In the turn phase, the majority of body rotation occurs about the inside limb. Finally, during the depart phase, the outside limb completes the rotation required to resume straight walking. In TD children, each phase reveals kinematic (Dixon et al., 2013) and kinetic (Dixon et al., 2014) adaptations with respect to straight walking.

The redirection of the COM during turning tasks is achieved via changes in amplitude or timing of muscle activations (Courtine & Schieppati, 2003b; Hase & Stein, 1999; Houck et al., 2007). Hase and Stein (1999) has provided a comprehensive analysis of spin turn muscle activations, albeit during changes in orientation of 180°. They presented a plausible interpretation of how muscles contribute to turning based on surface electromyographic (sEMG) muscle activation, but were unable to identify the relative contributions of each muscle to COM acceleration (Hase & Stein, 1999). Muscle induced segment acceleration is difficult to quantify based on muscle activations or net joint moments alone, especially for biarticular muscles, since a muscle can accelerate segments which it does not span (Zajac & Gordon, 1989; Zajac et al., 2003). Simulation using muscle actuated dynamic models can quantify the contributors to segment acceleration (Zajac et al., 2003) and reveal the mechanisms used to control COM movement. The goal of the 90° turn is to accelerate the COM in a direction perpendicular to the original walking direction. During straight walking, the COM acceleration perpendicular to the walking direction is controlled by the hip

abductors and ankle plantarflexors on the stance limb (medial and lateral COM acceleration, respectively) (Jansen et al., 2014; John et al., 2012; Pandy et al., 2010). These same muscles, as well as the hip adductors of the swing leg, are key drivers of COM acceleration perpendicular to the turning direction during circle walking (Ventura et al., 2015). It remains unclear if similar changes occur during the more common, transient spin turn manoeuvre.

Therefore, the aim of this study was to compare the role of muscles, gravity, and velocity-related forces in the modulation of COM acceleration perpendicular to the original straight walking direction during 90° pre-planned spin turns and straight walking in TD children. Based on the experimental setup, we analysed the approach (outside limb stance) and turn (inside limb stance) phase of the spin turn. The approach and turn phase of the spin turn were compared to corresponding phases of the gait cycle for straight walking (step 1 and 2, respectively of Fig. 1). We hypothesized that during the approach phase (1) outside limb hip abductors would increase their contribution to acceleration towards the turn side (medially) and (2) outside limb ankle plantarflexors would also show contribution towards the turn side (medially), instead of away from the turn side (laterally), compared to straight walking. For the turn phase, we hypothesized that (3), the contribution of the inside limb hip abductors to acceleration away from the turn side (medially) would decrease and (4) the inside limb ankle plantarflexors would further induce acceleration towards the turn side (laterally), compared to straight walking. Knowledge of complex, real-world tasks such as turning augments our understanding of gait and may lead to improvements in the management and treatment of gait deviations in populations with restricted gait ability.

2. Methods

2.1 Subjects, data collection and initial processing

Data from eleven TD children (11.2 ± 2.9 years, 151.2 ± 17.7 cm, 42.2 ± 10.8kg, 5 girls and 6 boys) performing straight walking and 90° turning gait trials (left and right) barefoot at self-selected speed were extracted from our laboratory database. Informed consent/assent for inclusion of data in further studies was obtained for all children. Analysis was limited to their preferred turning strategy (spin turn) (Fig.1).

A 12–16 camera system (Vicon Motion Systems Ltd., Oxford, UK) was used to collect data from the Plug-in Gait (PiG) (Kadaba et al., 1990) and Oxford Foot Model (Stebbins et al.,

2006) marker sets at 100 Hz. Additionally, the system synchronized data from force plates (Advanced Mechanical Technology Inc., Watertown, USA) embedded in the walkway and muscle activity patterns from sEMG electrodes (Wave, Cometa SrL., Milan, Italy) recorded at 1000 Hz. The sEMG electrodes were placed over the rectus femoris, semitendinosus, lateral gastrocnemius, and tibialis anterior. For four subjects, muscle activity from the posterior aspect of the gluteus medius was also collected. Identification of foot-off and foot-strike events, filtering of marker data, optimization of knee flexion/extension axis (Baker et al., 1999), and computation of joint kinematics and kinetics was conducted within the Nexus software environment (v1.7, Vicon Motion Systems Ltd., Oxford, UK). The data were imported into Matlab (v2011b, The Mathworks Inc., Natick, USA) where the raw sEMG data were smoothed using a 4th order zero-lag band-pass (10–500 Hz) Butterworth filter, averaged via the root mean square (50 ms window), and amplitude normalized to 100% of the signal. Moreover, v2 of the Lichtwark (2011) toolbox was used to generate input and set-up files (.mot, .trc, and .xml) from .c3d data for use in OpenSim (v3.1, Stanford, USA).

2.2 Musculo-skeletal modelling

Simulations were performed in OpenSim using the Gait2392 model and a dedicated workflow (Delp et al., 2007). Gait2392 comprises the upper body of the Anderson and Pandy (1999) model and the lower-limb model of Delp et al. (1990) with a knee model developed by Yamaguchi and Zajac (1989). This model has 23 degrees of freedom and 92 musculotendon actuators representing 76 muscles. The model subtalar and metatarsophalangeal joints were locked throughout the simulations. First, the generic model was scaled to the mass and dimensions of each subject via pairs of markers in the experimental static trial file and virtual markers appended to the generic model. In OpenSim, joint kinematics were obtained by minimizing a weighted squared error function between experimental and virtual markers defining anatomical landmarks (eq. 1 from Delp et al. (2007) with joint angle weighting factors set to zero) using the inverse kinematics tool. Joint kinetics were computed for the simulations from the inverse dynamics tool. Afterwards, a residual reduction algorithm reduced dynamic inconsistencies between model estimations and experimental ground reaction forces and a static optimization procedure estimated muscle activations (Delp et al., 2007). The performance criterion minimized the sum of the muscle activations squared (Crowninshield & Brand, 1981) and was constrained by the force-length-velocity characteristics of muscles (eq. 12 of Anderson and Pandy (2001)). Finally, an

induced acceleration analysis employing the roll kinematic constraint of Hamner (2010) determined the contribution of muscle, gravity, and velocity-related forces (Coriolis and centrifugal) to the COM medio-lateral acceleration. All accelerations were reported in a global referenced coordinate system (Fig. 1).

2.3 Comparison of experimental and simulated data

Figures for comparison of experimental and simulated spin turn data are presented within the manuscript (Figs. 2–7), while those for straight walking appear as supplemental material (Supplemental Figs 1–4). All comparisons between experimental and simulated data for spin turns were conducted for both limbs, normalized over all available time frames. For straight walking, data from the two sides were merged, assuming symmetry, to obtain a complete gait cycle, filtered to remove the discontinuity at the merger point, and normalized to 100%. OpenSim and Vicon inverse joint kinematics and kinetics generally showed good agreement via visual assessment (Figs. 2–5 and Supplemental Figs 1 and 2 for spin turns and straight walking, respectively). Originally, there was an offset between pelvic tilt values computed by the Gait2392 and PiG attributable to differences in the definition of the pelvic local coordinate system. The angle between the global horizontal and the vector formed by the sacral marker and the midpoint between the two anterior superior iliac spine markers was added to the Gait2392 hip sagittal plane angle values before comparison (NCSRR, 2014). For the PiG values, hip transverse plane data are more closely centered about zero, likely due to the adjustment of the thigh wand positions during the knee optimization procedure (Baker et al., 1999). For the residual reduction, remaining residuals were within acceptable limits (Hicks et al., 2015; NCSRR, 2014) with root mean square (RMS) maximum and average values of 16.7 and 3.5 N, respectively, for the forces and maximum and average RMS of 33.2 and 0.94 Nm, respectively, for the moments. Translational (position) RMS errors were 1.3 cm, while rotational (joint angle) RMS errors were negligible. Visual comparison of the calculated muscle activations via static optimization with experimental sEMG data revealed good overall agreement; however, it was noted that the gluteus medius remained active longer than expected during simulations (Winter & Yack, 1987) (Fig. 6 and Supplemental Fig. 3 for spin turns and straight walking, respectively). No attempt was made to add additional constraints to improve agreement, as the effect would be similar across conditions and not alter the study conclusions. For the induced acceleration analysis, comparison of the sum of each contributor to the COM acceleration and the twice-differentiated positions of the

simulated (superposition) and experimental COM showed good agreement (Fig. 7 and Supplemental Fig. 4 for spin turn and straight walking, respectively).

2.4 Further processing and statistical analysis

Trials were separated into approach and turn phases. The approach phase begins in single limb support of the outside limb and ends at outside limb foot-off. The turn phase only comprises single-limb support of the inside limb (Fig. 1). Together, on average, these phases accounted for 57° of the total turn (measured by the change in pelvis transverse plane angle). Only accelerations in the direction perpendicular to the original walking direction were analysed. Acceleration is referenced as towards (negative) or away from (positive) the turn side. Thus, acceleration lateral to the outside limb (or first step) and medial to the inside limb (or second step), is positive.

The acceleration of the COM (sum of all contributors) and each individual contributor across conditions (spin vs straight) averaged over each step (outside or first and inside or second) was extracted for each subject. Any average contribution less than 0.01 m/s^2 was arbitrarily considered as negligible and not analysed; however, if anatomically meaningful, these small contributors were grouped (Jansen et al., 2014; Pandy et al., 2010) and reassessed for inclusion in the analysis based on the above criterion (Table 1).

Normality and homogeneity of variance was assessed by visualisation of QQ–plots and Levene's test, respectively. Deviations from either parametric assumption led to the use of the Wilcoxon Signed Rank test; otherwise, paired t-tests were implemented. No corrections to p-values for multiple tests were made (Feise, 2002). Significance level was set at $\alpha = 0.05$. Effect size, Cohen's d (d) or Glass's delta (Δ), was also computed for parametric and non-parametric tests, respectively. Error variances were non-homogeneous for total COM, inside MGAS, inside LGAS, and inside SOL during the turn phase.

3. Results

3.1 Global medio-lateral centre of mass acceleration

During the approach phase, the COM acceleration towards the turn side increased during spin turns (-0.93 m/s^2) compared to straight walking (-0.34 m/s^2) ($p < 0.001$ and d =

2.29) (Fig. 8 a). During the turn phase, the COM continued to be accelerated towards the turn side for spin turns (-0.88 m/s^2), but was oriented medially with respect to the inside limb (second step) for straight walking (0.36 m/s^2) ($p < 0.001$ and $\Delta = 8.60$) (Fig. 8 b).

3.2. Contributors to global medio-lateral centre of mass acceleration

For the approach phase of straight walking and spin turns, the outside GMED, GMIN, SOL, MGAS, and ILIPSO, as well as gravity were the largest contributors to COM acceleration perpendicular to the straight walking direction (Fig. 8 a). Contribution to COM acceleration was reduced during spin turns compared to straight walking for outside SOL (0.01 vs 0.29, m/s^2, $p < 0.001$, and $d = 2.16$) and outside MGAS (0.01 vs 0.19 m/s^2, $p < 0.001$, and $d = 2.41$); however, contribution to COM acceleration was increased for gravity during spin turns (-0.12 m/s^2) compared to straight walking (-0.07 m/s^2) ($p < 0.001$, and $d = 1.64$).

For the turn phase, inside GMED, GMIN, SOL, MGAS, LGAS, and VAS were the greatest contributors to COM acceleration perpendicular to the straight walking direction (Fig. 8 b). Contribution to COM acceleration was reduced during spin turns compared to straight walking for inside GMED (0.43 vs 0.73 m/s^2, $p < 0.001$, and $d = 2.36$), inside GMIN (0.10 vs 0.15 m/s^2, $p < 0.001$, and $d = 1.72$) and inside VAS (0.01 vs -0.12 m/s^2, $p = 0.001$, and $d = 1.61$). Contributions to COM acceleration were increased during spin turns compared to straight walking for inside SOL (-0.66 vs -0.30 m/s^2, $p = 0.014$, and $\Delta = 6.00$), inside MGAS (-0.56 vs -0.19 m/s^2, $p = 0.002$, and $\Delta = 4.50$), and inside LGAS (-0.12 vs -0.04, $p = 0.001$, and $\Delta = 4.56$).

4. Discussion

The purpose of this study was to determine the role of muscles, gravity and velocity-related forces in the control and redirection of the COM during 90° spin turns. An induced acceleration analysis revealed that TD children mainly modulate hip abductor and ankle plantarflexor contributions to COM acceleration towards the new walking direction.

4.1 Control of centre of mass acceleration

During straight walking, the medio-lateral COM position oscillates sinusoidally at the stride frequency rate and is directed towards the stance limb (Inman et al., 2006). This motion

is controlled by acceleration that tends to pull the COM back towards the body midline with each step (Jansen et al., 2014; Pandy et al., 2010). Muscle contributions to global medio-lateral COM acceleration presented here agree with previous investigators: hip abductors and ankle plantarflexors tend to contribute to and oppose COM medio-lateral acceleration, respectively (Jansen et al., 2014; Pandy et al., 2010).

For spin turns, we proposed two hypotheses for each phase under analysis. For the approach, we posited that outside hip abductors would increase contribution towards the turn side, while outside ankle plantarflexors would switch from an opposing (away from the turn side) to a supporting (towards the turn side) acceleration contribution, compared to straight walking. These hypotheses were not confirmed. Instead, outside GMED and outside GMIN contributions during spin turns remained similar to straight walking, resulting in an increased acceleration towards the turn side only via a reduction of outside SOL and outside MGAS contributions. In other words, turning appears to be initiated only by a reduction in muscle contribution, possibly representing a more efficient use of muscles than the paradigm we proposed. For the turn phase, our hypotheses were confirmed: inside GMED and inside GMIN contribution away from the turn side was reduced, while inside SOL, MGAS, and LGAS acceleration contributions towards the turn side were increased, compared to straight walking. The hip abductor contribution to acceleration away from the turn side may occur to avoid an increase in hip adduction and maintain pelvis stability during turning (Hase & Stein, 1999), regardless of its opposition to the task of accelerating the COM towards the turn side. The increased contribution of the ankle plantarflexors may also have helped to reaccelerate the COM in the forward direction; however, similar ankle power generation across tasks would suggest that this may not be the case (Dixon et al., 2014).

Previous turning gait studies focused on COM kinematics have mainly been descriptive. In the work of Patla et al. (1999), redirection of the COM position was attributed to changes in foot placement and trunk motion, but how subjects modulated muscle activity to achieve these new postures remained unclear. Later, Xu et al. (2004) found that the COM to centre of pressure distance was modulated in an anticipatory fashion (during the step before the turn, i.e., the approach step) as a way to "initiate the disequilibrium necessary to produce the turn". Here, using an induced acceleration analysis, not only were anticipatory effects noted (change in COM approach phase acceleration), but the muscles responsible could also be identified and their contributions quantified.

To date, a single simulation-based induced acceleration analysis of a turning task (circle walking) has been reported (Ventura et al., 2015). The current findings for the hip abductors and ankle plantarflexors are in agreement with this work; however, additional contribution away from the turn by the inside leg hip adductors during swing were reported as important (Ventura et al., 2015). Action of the hip adductors was not investigated here since these muscles contributed minimally to the overall COM acceleration (< 0.01 m/s^2). It is possible that the more dynamic nature of the spin turn, in comparison to circle walking, results in a decreased reliance on these smaller muscles. Notably, Ventura et al. (2015) suggested that differences in muscle contributions to COM acceleration across conditions may depend less on differences in muscle force and more on differences in the orientation of the segments during each task. This might help explain the apparent disagreement with past electromyography-based experiments (Courtine et al., 2006; Duval et al., 2011).

4.2 Limitations

Five limitations warrant further discussion. Firstly, the results suggest that the majority of the medio-lateral acceleration in spin turns occurs during the approach phase (COM acceleration of -0.93 and -0.88 m/s^2 for the approach and turn phase, respectively) (Fig. 8); however, it is likely that additional acceleration is gained during inside limb pre-swing via the ankle plantarflexor push-off power generation burst. Unfortunately, it was not possible to record this information given our experimental set-up. Force plates positioned along the turning path or methods in which force plate data are simulated (Fluit et al., 2014) could have allowed for investigation of a complete turn (approach, turn, and depart phases). Secondly, the rolling constraint of the foot-ground contact model used in the induced acceleration analysis does not allow for twisting of the foot about the global vertical axis (Hamner et al., 2013). Nonetheless, the constraint was favoured since in our previous work peak torques during spin turns, although increased, were of a similar order of magnitude to those of straight walking (78.9 vs 56.0 N mm/kg) (Dixon et al., 2014) and other models (point and weld constraint) have been shown to less adequately reproduce experimental ground reaction forces, leading to erroneous acceleration contributions (Hamner et al., 2013). Thirdly, in TD children, spins turns result in a reduction in gait speed, compared to straight walking (Dixon et al., 2013). Therefore, some of the observed differences across tasks may be related to speed; however, similar changes were reported in the study of Ventura et al. (2015) in which speed was controlled across tasks. Fourthly, given the limited validation for muscle control at the subtalar joint, it was locked during simulations as in Liu et al. (2008),

possibly impacting the contributions of the ankle plantarflexors reported herein. An investigation of the effect of unlocking the subtalar joint on the contributors to medio-lateral COM acceleration during spin turns was attempted; however, muscle activation patterns themselves, particularly for the inside limb tibialis anterior (Supplemental Fig. 5 c), were found to less accurately reproduce the experimental patterns (sEMG), compared to the locked version. Finally, the scope of this paper did not encompass antero-posterior and vertical COM acceleration analysis. Visualization of the overall COM accelerations in these planes showed relatively minor differences across conditions (Supplemental Fig. 6) and thus they were not investigated further.

4.3 Conclusions

Our analysis reveals that TD children modulate proximal and distal leg muscle contributions during spin turns to redirect the COM. This strategy may challenge stability and it is unknown if children with gait disabilities, such as children with cerebral palsy, would adapt similarly as they often present with decreased balance, weak hip abductors and weak ankle plantarflexors. Future investigations of adaptive turning strategies using an induced acceleration analysis could lead to improvements in the management of gait disorders.

5. Acknowledgements

The first author acknowledges support from the Fonds de Recheche du Québec – Santé Doctoral Training Award and the Gustav Born Scholarship at St Peter's College, Oxford. Travel of first author to Belgium for this study was funded by the St Peter's College Graduate Fund. All authors acknowledge the Oxford Gait Laboratory clinical staff for help with collection and initial data processing.

6. References

Anderson, F. C., & Pandy, M. G., 1999. A Dynamic Optimization Solution for Vertical Jumping in Three Dimensions. Comput Methods Biomech Biomed Engin, 2(3), 201-231.

Anderson, F. C., & Pandy, M. G., 2001. Static and dynamic optimization solutions for gait are practically equivalent. J Biomech, 34(2), 153-161.

Baker, R., Finney, L., & Orr, J., 1999. A new approach to determine the hip rotation profile from clinical gait analysis data. Hum Mov Sci, 18(5), 655-667.

Courtine, G., Papaxanthis, C., & Schieppati, M., 2006. Coordinated modulation of locomotor muscle synergies constructs straight-ahead and curvilinear walking in humans. Exp Brain Res, 170(3), 320-335.

Courtine, G., & Schieppati, M., 2003a. Human walking along a curved path. I. Body trajectory, segment orientation and the effect of vision. Eur J Neurosci, 18(1), 177-190.

Courtine, G., & Schieppati, M., 2003b. Human walking along a curved path. II. Gait features and EMG patterns. Eur J Neurosci, 18(1), 191-205.

Crowninshield, R. D., & Brand, R. A., 1981. A Physiologically Based Criterion of Muscle Force Prediction in Locomotion. J Biomech, 14(11), 793-801.

Delp, S. L., Anderson, F. C., Arnold, A. S., Loan, P., Habib, A., John, C. T., Guendelman, E., & Thelen, D. G., 2007. Open{S}im: Open-source software to create and analyze dynamic Simulations of movement. IEEE Trans Biomed Eng, 54(11), 1940-1950.

Delp, S. L., Loan, J. P., Hoy, M. G., Zajac, F. E., Topp, E. L., & Rosen, J. M., 1990. An interactive graphics-based model of the lower extremity to study orthopaedic surgical procedures. IEEE Trans Biomed Eng, 37(8), 757-767.

Desloovere, K., Wong, P., Swings, L., Callewaert, B., Vandenneucker, H., & Leardini, A., 2010. Range of motion and repeatability of knee kinematics for 11 clinically relevant motor tasks. Gait Posture, 32(4), 597-602.

Dixon, P. C., Stebbins, J., Theologis, T., & Zavatsky, A. B., 2013. Spatio-temporal parameters and lower-limb kinematics of turning gait in typically developing children. Gait Posture, 38(4), 870-875.

Dixon, P. C., Stebbins, J., Theologis, T., & Zavatsky, A. B., 2014. Ground reaction forces and lower-limb joint kinetics of turning gait in typically developing children. J Biomech, 47(15), 3726-3733.

Duval, K., Luttin, K., & Lam, T., 2011. Neuromuscular strategies in the paretic leg during curved walking in individuals post-stroke. J Neurophysiol, 106(1), 280-290.

Feise, R. J., 2002. Do multiple outcome measures require p-value adjustment? BMC Med Res Methodol, 2, 8.

Fluit, R., Andersen, M. S., Kolk, S., Verdonschot, N., & Koopman, H. F., 2014. Prediction of ground reaction forces and moments during various activities of daily living. J Biomech, 47(10), 2321-2329.

Glaister, B. C., Bernatz, G. C., Klute, G. K., & Orendurff, M. S., 2007. Video task analysis of turning during activities of daily living. Gait Posture, 25(2), 289-294.

Glaister, B. C., Orendurff, M. S., Schoen, J. A., Bernatz, G. C., & Klute, G. K., 2008. Ground reaction forces and impulses during a transient turning maneuver. J Biomech, 41(14), 3090-3093.

Grasso, R., Prevost, P., Ivanenko, Y. P., & Berthoz, A., 1998. Eye-head coordination for the steering of locomotion in humans: An anticipatory synergy. Neurosci Lett, 253(2), 115-118.

Hamner, S. R., Seth, A., & Delp, S. L., 2010. Muscle contributions to propulsion and support during running. J Biomech, 43(14), 2709-2716.

Hamner, S. R., Seth, A., Steele, K. M., & Delp, S. L., 2013. A rolling constraint reproduces ground reaction forces and moments in dynamic simulations of walking, running, and crouch gait. J Biomech, 46(10), 1772-1776.

Hase, K., & Stein, R. B., 1999. Turning strategies during human walking. J Neurophysiol, 81(6), 2914-2922.

Hicks, J. L., Uchida, T. K., Seth, A., Rajagopal, A., & Delp, S. L., 2015. Is My Model Good Enough? Best Practices for Verification and Validation of Musculoskeletal Models and Simulations of Movement. Journal of Biomechanical Engineering-Transactions of the Asme, 137(2).

Houck, J. R., Wilding, G. E., Gupta, R., De Haven, K. E., & Maloney, M., 2007. Analysis of EMG patterns of control subjects and subjects with ACL deficiency during an unanticipated walking cut task. Gait Posture, 25(4), 628-638.

Inman, V. T., Ralston, H. J., & Todd, F., (2006). Human locomotion. In J. Rose & J. G. Gamble (Eds.), Human Walking

Jansen, K., De Groote, F., Duysens, J., & Jonkers, I., 2014. How gravity and muscle action control mediolateral center of mass excursion during slow walking: A simulation study. Gait Posture, 39(1), 91-97.

John, C. T., Seth, A., Schwartz, M. H., & Delp, S. L., 2012. Contributions of muscles to mediolateral ground reaction force over a range of walking speeds. J Biomech, 45(14), 2438-2443.

Kadaba, M. P., Ramakrishnan, H. K., & Wootten, M. E., 1990. Measurement of lower extremity kinematics during level walking. J Orthop Res, 8(3), 383-392.

Lichtwark, G. (2011). Matlab OpenSim Pipeline Tools v2 (Version 2).

Liu, M. Q., Anderson, F. C., Schwartz, M. H., & Delp, S. L., 2008. Muscle contributions to support and progression over a range of walking speeds. J Biomech, 41(15), 3243-3252.

NCSRR. (2014). OpenSim Best Practices. Retrieved December 18th, 2014, from http://opensim.stanford.edu/support/

Pandy, M. G., Lin, Y. C., & Kim, H. J., 2010. Muscle coordination of mediolateral balance in normal walking. J Biomech, 43(11), 2055-2064.

Patla, A. E., Adkin, A., & Ballard, T., 1999. Online steering: Coordination and control of body center of mass, head and body reorientation. Exp Brain Res, 129(4), 629-634.

Patla, A. E., Prentice, S. D., Robinson, C., & Neufeld, J., 1991. Visual control of locomotion: Strategies for changing direction and for going over obstacles. J Exp Psychol Hum Percept Perform, 17(3), 603-634.

Sedgman, R., Goldie, P., & Iansek, R., 1994. Development of a measure of turning during walking. In Proc. of the 1st Advancing rehabilitation conference. Melbourne, Australia.

Stebbins, J., Harrington, M., Thompson, N., Zavatsky, A. B., & Theologis, T., 2006. Repeatability of a model for measuring multi-segment foot kinematics in children. Gait Posture, 23(4), 401-410.

Strike, S. C., & Taylor, M. J., 2009. The temporal-spatial and ground reaction impulses of turning gait: Is turning symmetrical? Gait Posture, 29(4), 597-602.

Taylor, M. J., Dabnichki, P., & Strike, S. C., 2005. A three-dimensional biomechanical comparison between turning strategies during the stance phase of walking. Hum Mov Sci, 24(4), 558-573.

Ventura, J. D., Klute, G. K., & Neptune, R. R., 2015. Individual muscle contributions to circular turning mechanics. J Biomech.

Winter, D. A., & Yack, H. J., 1987. EMG profiles during normal human walking: Stride-to-stride and inter-subject variability. Electroencephalogr Clin Neurophysiol, 67(5), 402-411.

Xu, D., Carlton, L. G., & Rosengren, K. S., 2004. Anticipatory postural adjustments for altering direction during walking. J Mot Behav, 36(3), 316-326.

Yamaguchi, G. T., & Zajac, F. E., 1989. A planar model of the knee joint to characterize the knee extensor mechanism. J Biomech, 22(1), 1-10.

Zajac, F. E., & Gordon, M. E., 1989. Determining muscle's force and action in multi-articular movement. Exerc Sport Sci Rev, 17, 187-230.

Zajac, F. E., Neptune, R. R., & Kautz, S. A., 2003. Biomechanics and muscle coordination of human walking. Part II: Lessons from dynamical simulations and clinical implications. Gait Posture, 17(1), 1-17.

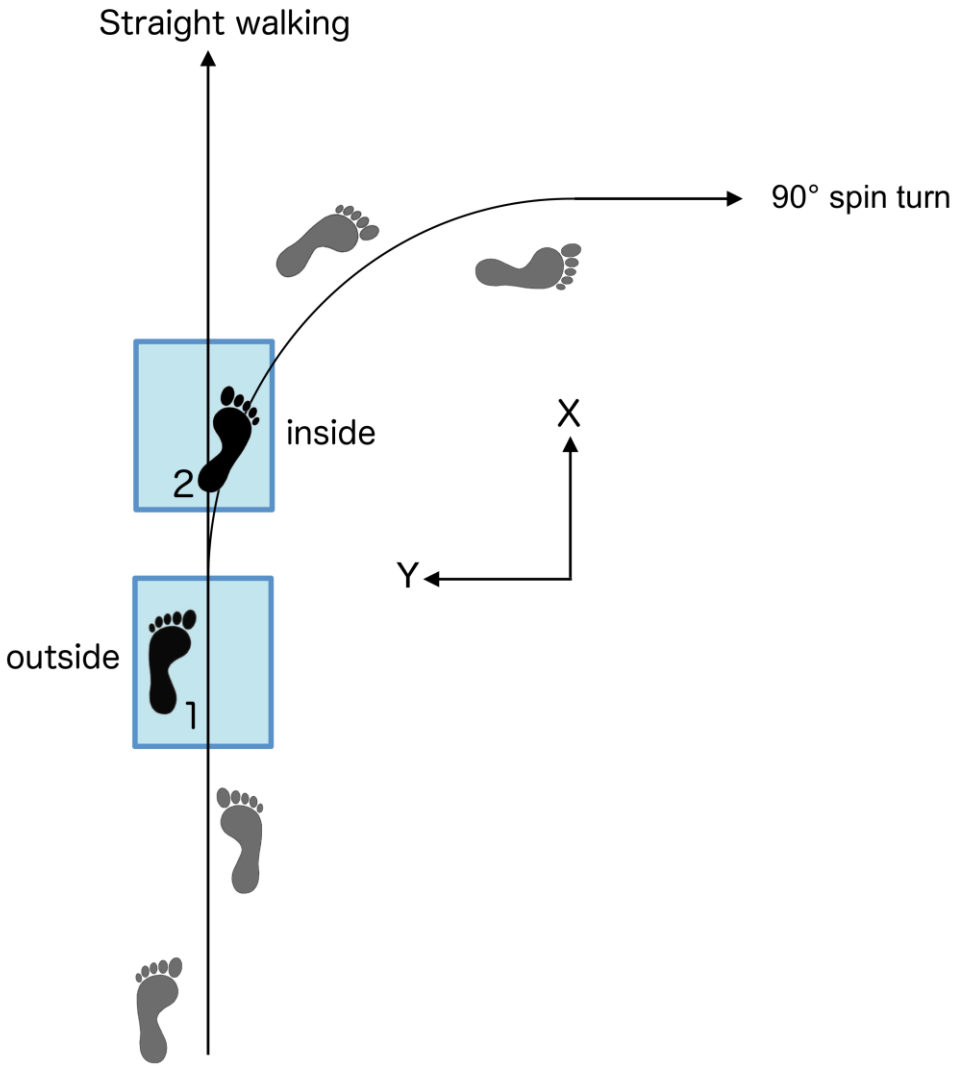

Fig. 1: Diagrammatic representation of a 90° spin turn to the right and a straight walking trial. Shaded rectangles represent force plates embedded in the walking surface. The approach phase begins in single limb support of the outside limb (step 1, left black footprint) and ends at the start of single-limb support of the inside limb (step 2, right black footprint). The turn phase only comprises single-limb support of the inside limb. The approach and turn phase of the spin turn were compared to step 1 and 2, respectively, for straight walking. Steps not analysed shown in grey. Only accelerations in the direction perpendicular to the original walking direction (global Y direction) were analysed. Acceleration lateral to the outside limb and medial to the inside limb (away from the turn direction) are positive.

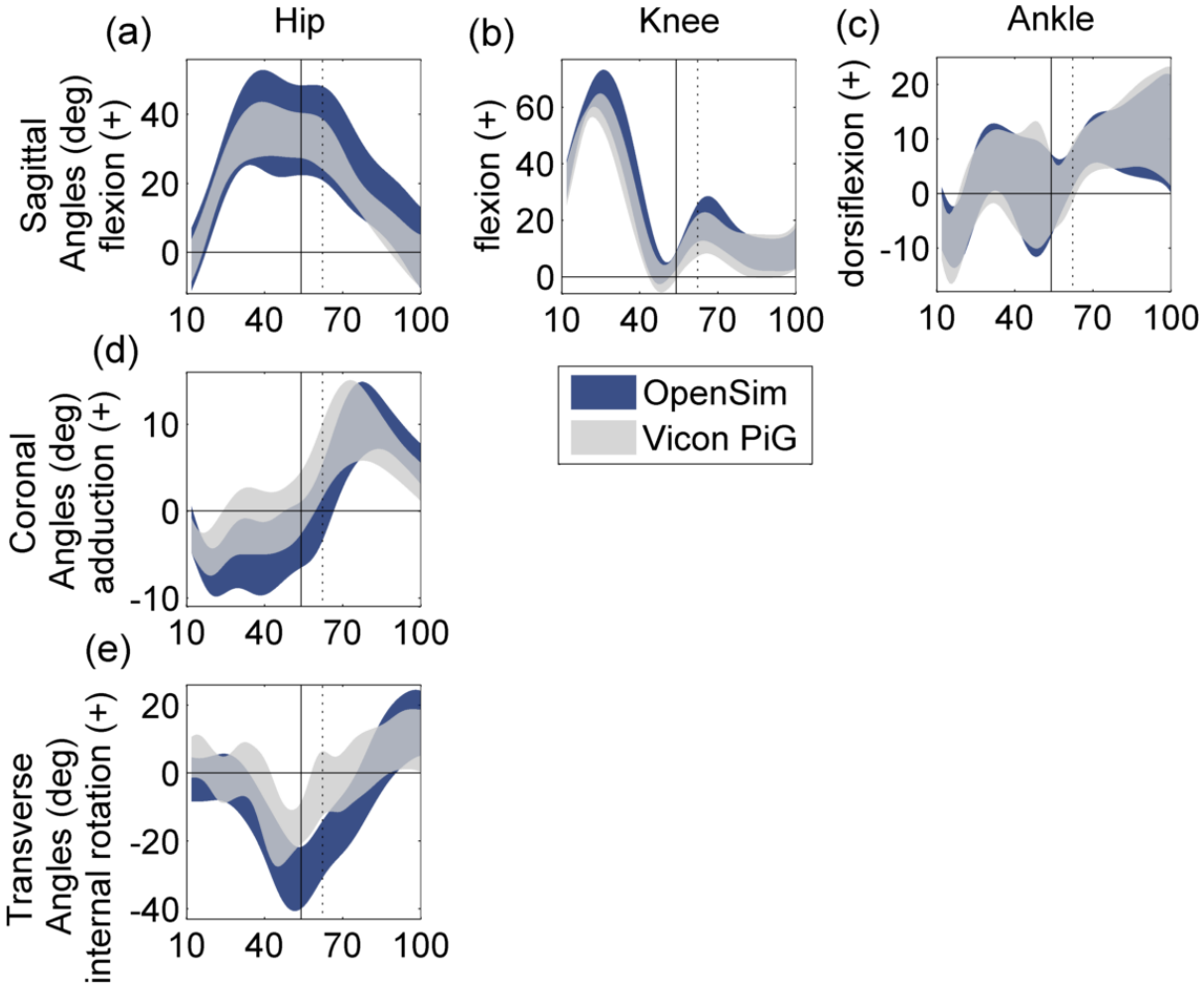

Fig. 2: Inside limb hip (a, d, and e), knee (b), and ankle (c) joint kinematics during spin turns (x–axis: 12–100% of the gait cycle) with solid and dashed vertical lines at inside foot-strike and outside foot-off, respectively. Standard deviation band of simulated (OpenSim) and experimental plug-in gait (Vicon PiG) kinematics shown. Only sagittal plane ankle and knee data presented as musculo-skeletal model subtalar joint was locked for simulation and knee has a single flexion/extension axis, respectively.

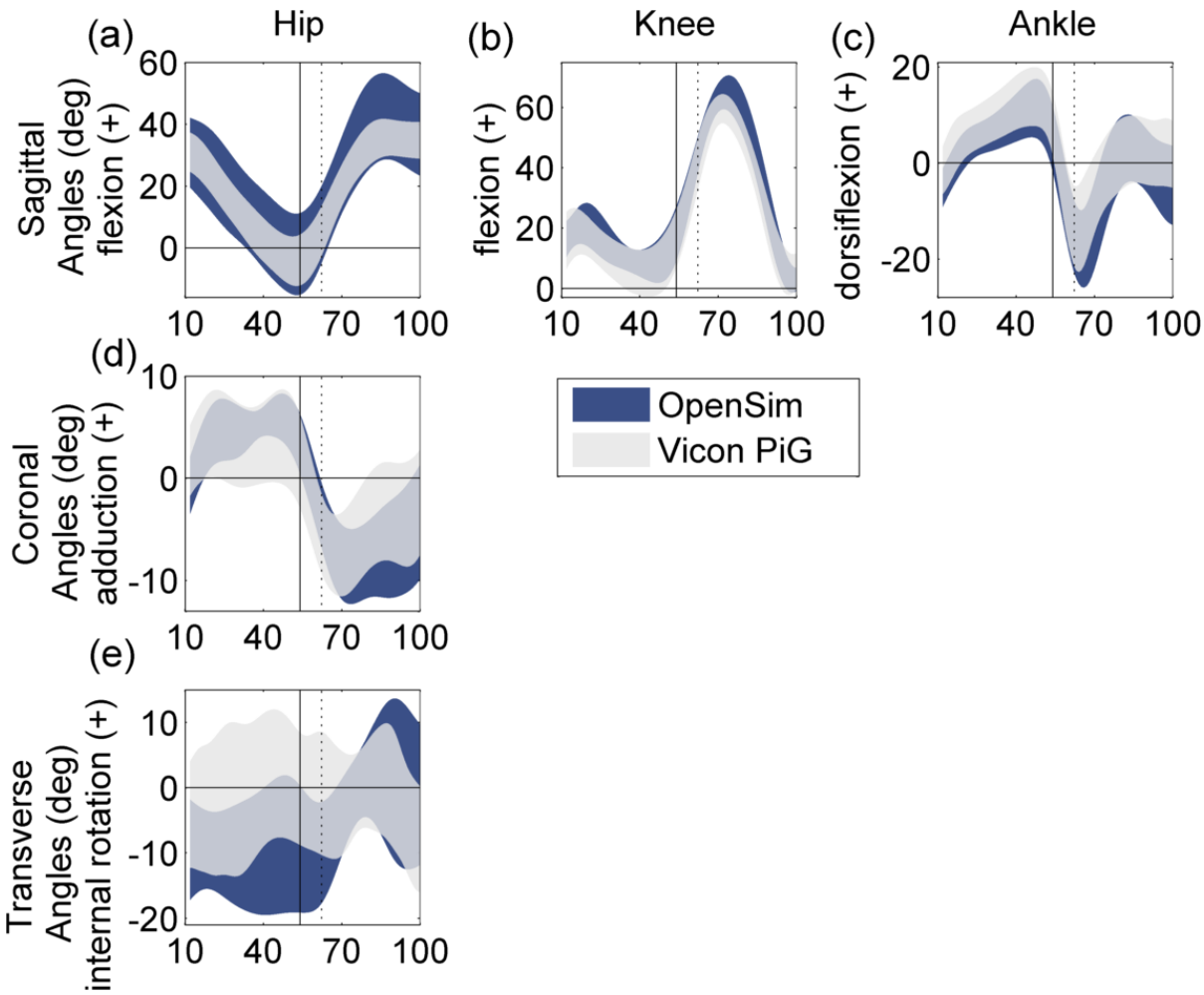

Fig. 3: Outside limb hip (a, d, and e), knee (b), and ankle (c) joint kinematics during spin turns (x–axis: 12–100% of the gait cycle) with solid and dashed vertical lines at inside foot-strike and outside foot-off, respectively. Standard deviation band of simulated (OpenSim) and experimental plug-in gait (Vicon PiG) kinematics shown. Only sagittal plane ankle and knee data presented as musculo-skeletal model subtalar joint was locked for simulation and knee has a single flexion/extension axis, respectively.

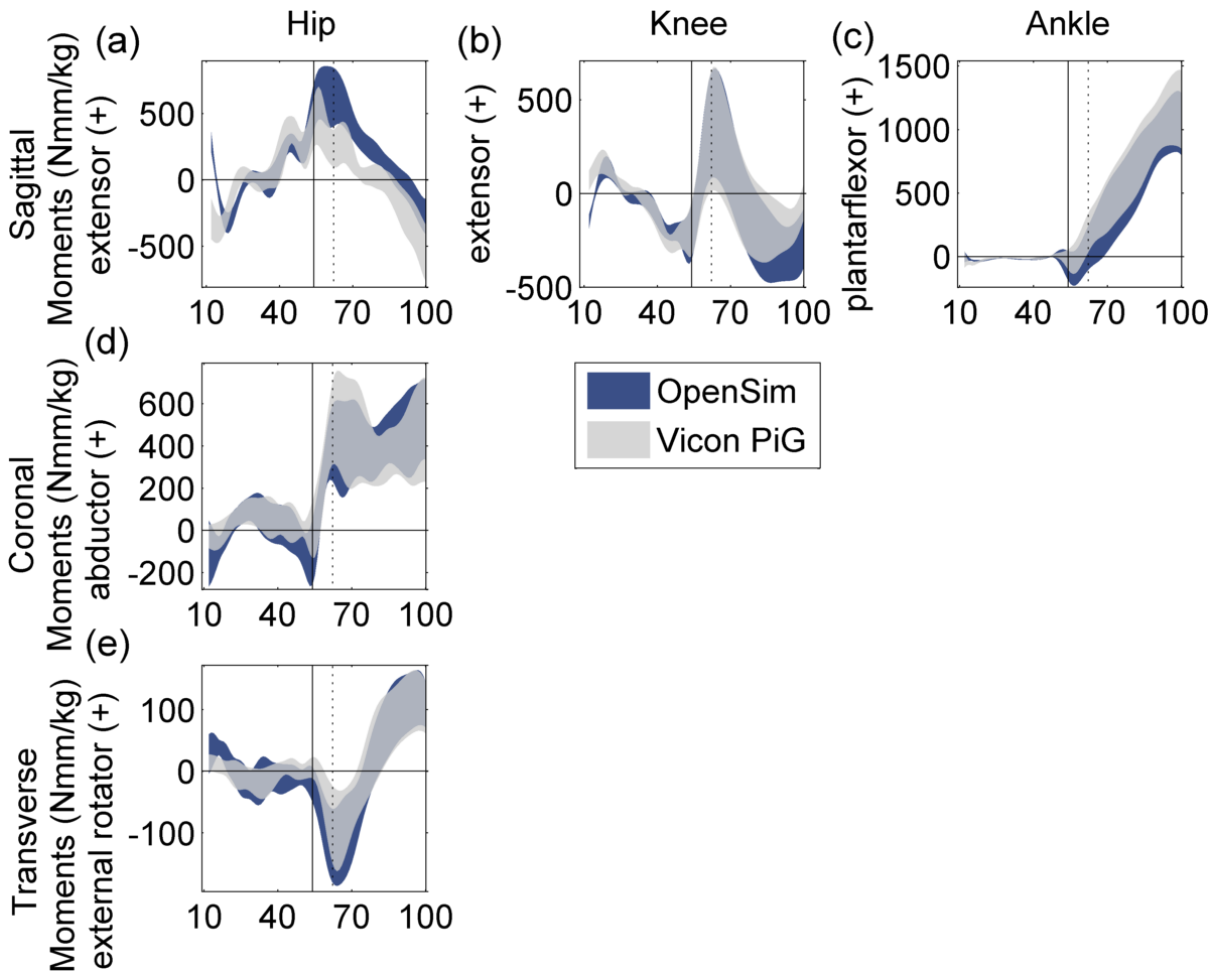

Fig. 4: Inside limb hip (a, d, and e), knee (b), and ankle (c) joint moments during spin turns (x–axis: 12–100% of the gait cycle) with solid and dashed vertical lines at inside foot-strike and outside foot-off, respectively. Standard deviation band of simulated (OpenSim) and experimental plug-in gait (Vicon PiG) kinetics shown. Only sagittal plane ankle and knee data presented as musculo-skeletal model subtalar joint was locked for simulation and knee has a single flexion/extension axis, respectively.

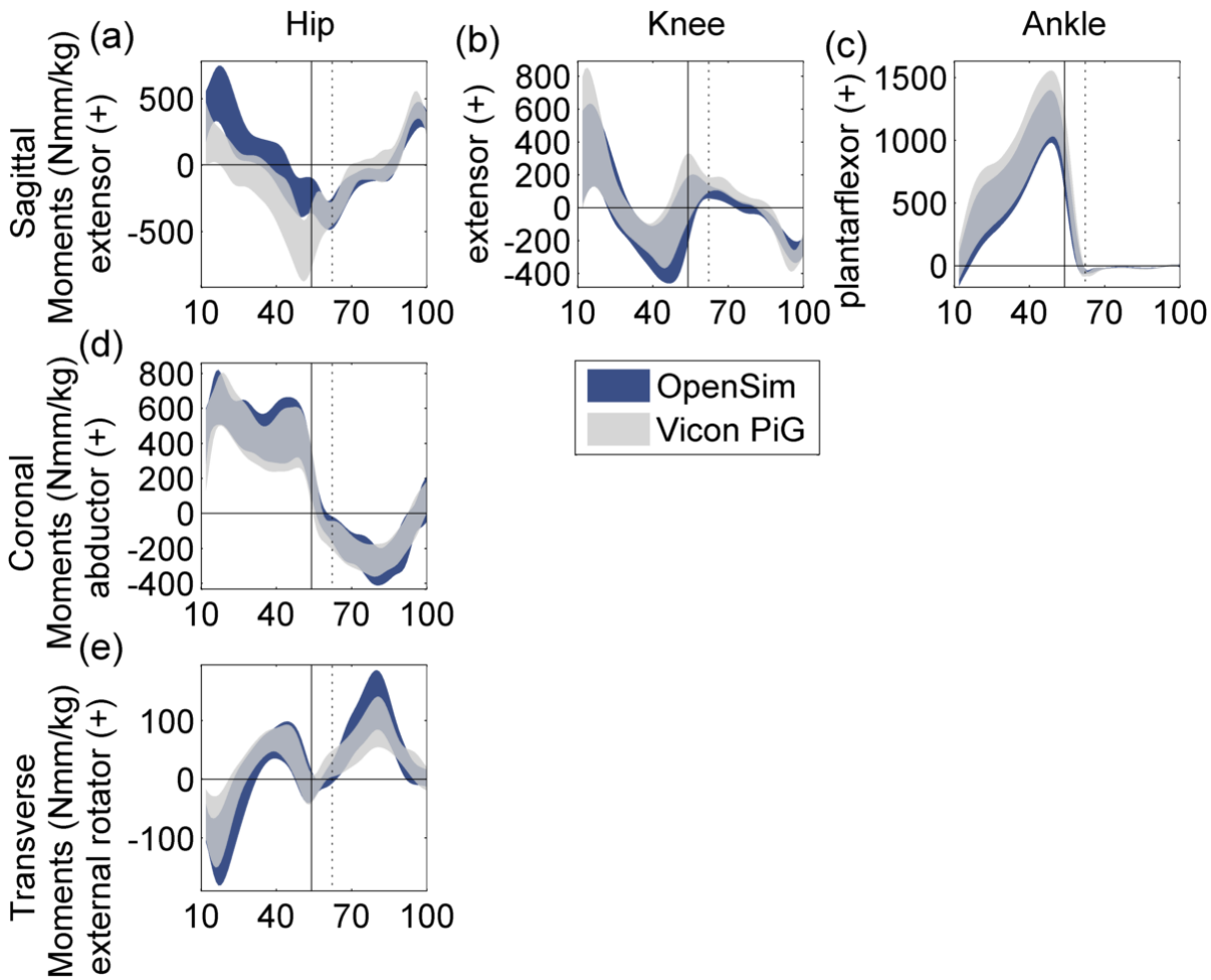

Fig. 5: Outside limb hip (a, d, and e), knee (b), and ankle (c) joint moments during spin turns (x–axis: 12–100% of the gait cycle) with solid and dashed vertical lines at inside foot-strike and outside foot-off, respectively. Standard deviation band of simulated (OpenSim) and experimental plug-in gait (Vicon PiG) kinetics shown. Only sagittal plane ankle and knee data presented as musculo-skeletal model subtalar joint was locked for simulation and knee has a single flexion/extension axis, respectively.

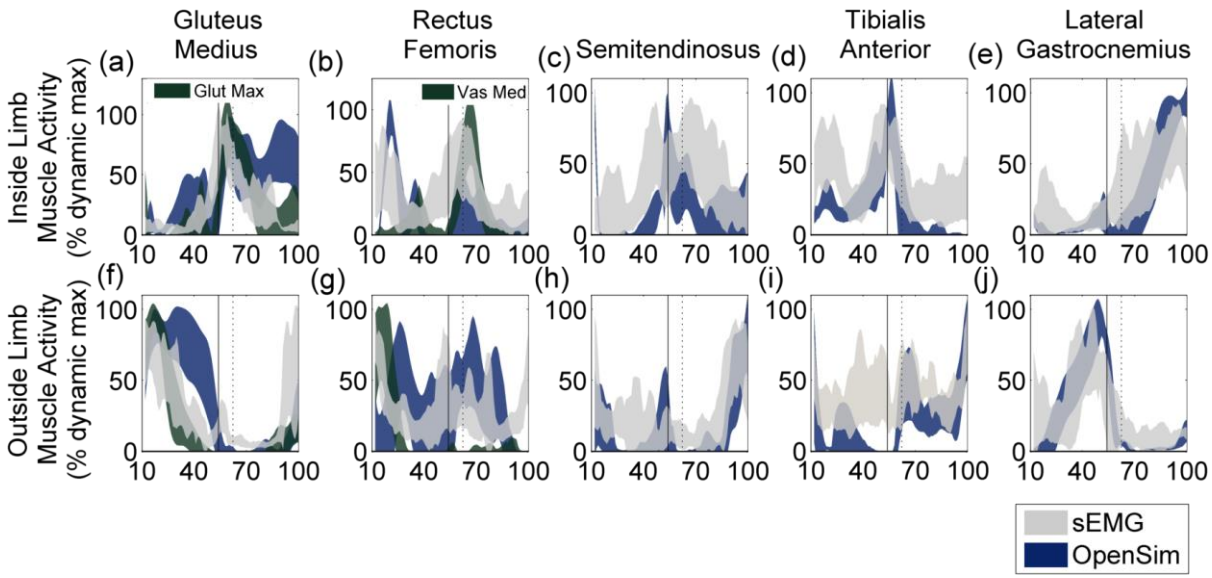

Fig. 6: Inside (top) and outside (bottom) limb muscle activity during spin turns (x–axis: 12–100% of the gait cycle) with solid and dashed vertical lines at inside foot-strike and outside foot-off, respectively. Standard deviation band of simulated (OpenSim) and processed surface electromyographic (sEMG) data presented for (a and f) Gluteus Medius, (b and g) Rectus Femoris, (c and h) Semitendinosus, (d and i) Tibialis Anterior, and (e and j) Lateral Gastrocnemius. For (a and f) and (b and g) simulated muscle activity from Gluteus Maximus (Glut Max) and Vastus Medialis (Vast Med), respectively, also shown. Gluteus Medius activity recorded for n = 4 subjects.

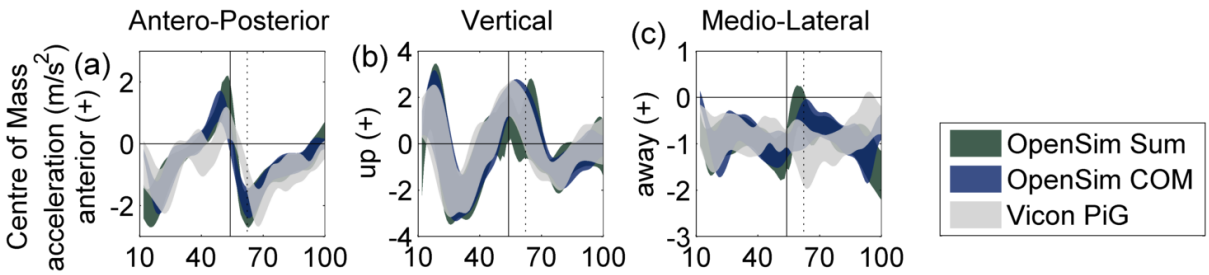

Fig. 7 Centre of mass (COM) acceleration in the (a) antero-posterior, (b) vertical, and (c) medio-lateral direction during spin turns (x–axis: 12–100% of the gait cycle) with solid and dashed vertical lines at inside foot-strike and outside foot-off, respectively. Standard deviation band of all muscle accelerations (OpenSim Sum), second derivative of COM position from simulations (OpenSim COM), and second derivative of plug-in gait model COM position (Vicon PiG) shown.

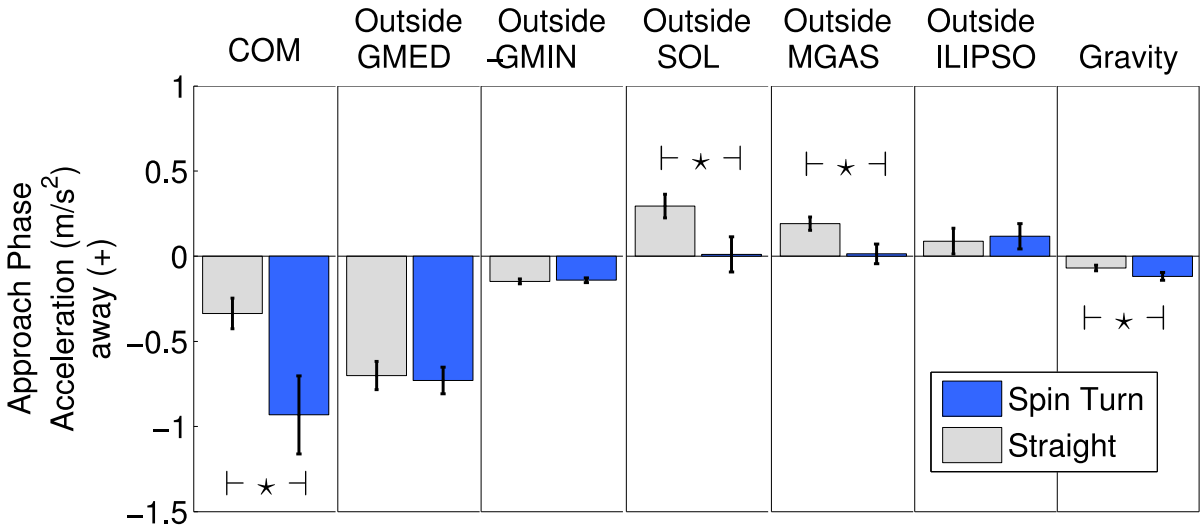

(a)

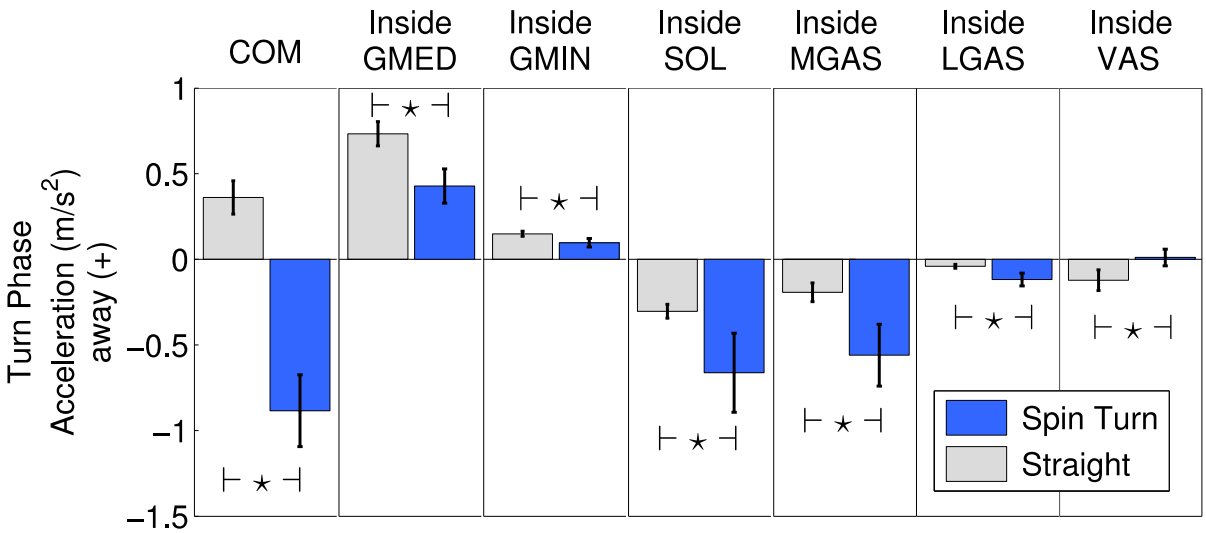

(b)

Fig. 8: Medio-lateral acceleration of the centre of mass (COM) and main contributors across conditions (straight and spin turns) for the (a) approach and (b) turn phase. During the approach phase, the outside and inside limbs are in stance and swing, respectively. During the turn phase, inside and outside limbs are in stance and swing, respectively. Significant difference at $\alpha = 0.05$ level shown (★). See Table 1 for muscle abbreviations. Bar graphs show means and confidence intervals. Acceleration lateral to the outside limb (first step) and medial to the inside limb (second step) (away from the turn side), positive (see Fig. 1).

Table 1: Muscle groups and abbreviations

Abbreviation	Description
ADD	Adductor longus, brevis, and magnus (3 actuators)
DF	Tibialis anterior, extensor digitorum, and extensor hallucis
GMAX	Gluteus maximus (anterior, medial, and posterior actuators)
GMED	Gluteus medius (anterior, medial, and posterior actuators)
GMIN	Gluteus minimus (anterior, medial, and posterior actuators)
HAMS	Semimembranosus, semitendinosus, bicep femoris long head
ILIPSO	Iliacus and psoas
LGAS	Lateral head of gastrocnemius
MGAS	Medial head of the gastrocnemius
PFEV	Peroneus brevis, peroneus longus, peroneus tertius
PFIN	Tibialis posterior, flexor digitorum, flexor hallucis
SOL	Soleus
VAS	Vastus intermedius, medialis, and lateralis

ADD, DF, GMAX, HAMS, PFEV, and PFIN groups not statistically analysed as contributions to overall medio-lateral COM acceleration were less than 0.1 m/s^2.

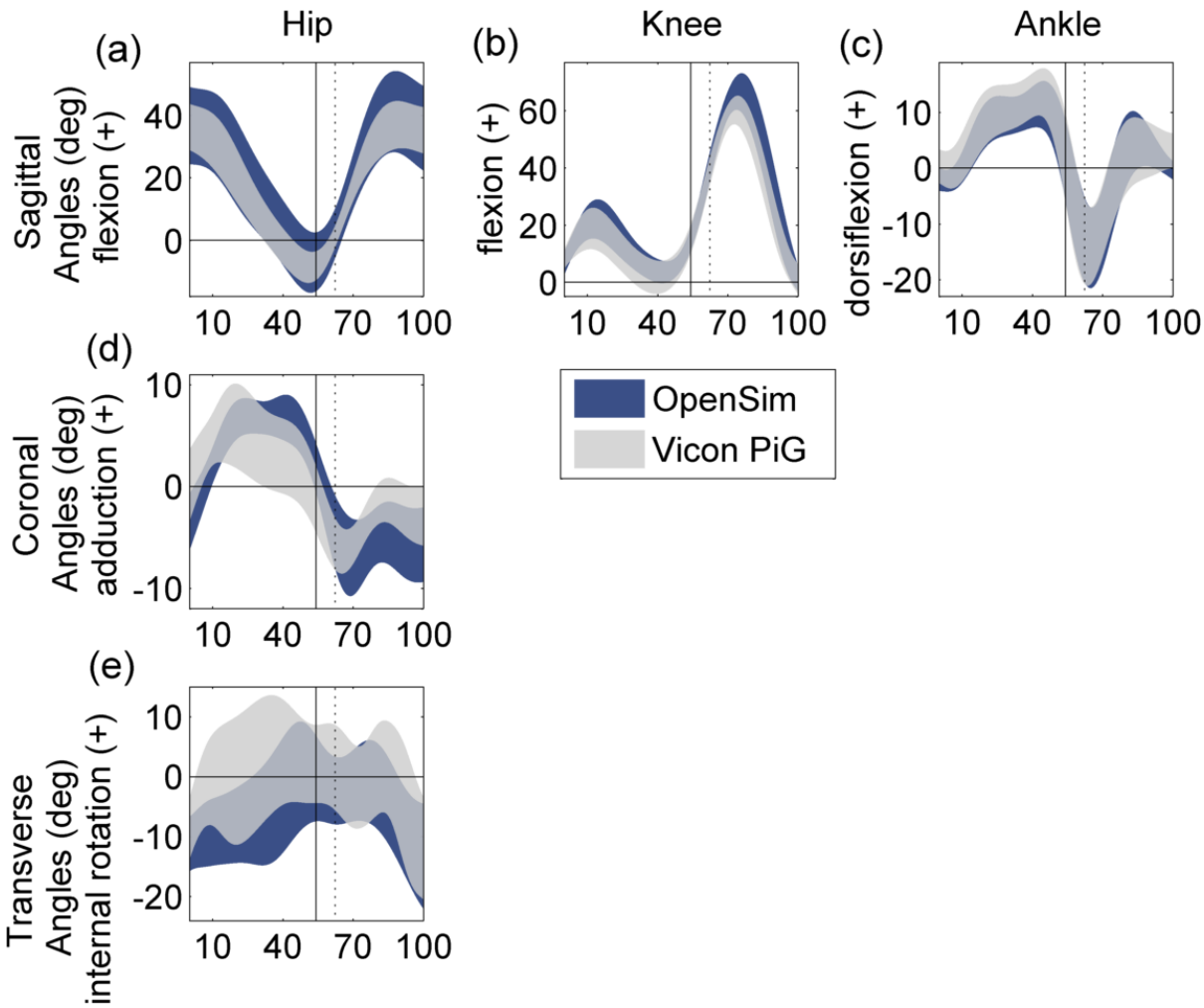

Supplemental Fig.1: Hip, knee, and ankle joint kinematics during straight walking (x–axis: 0–100% of the gait cycle) with solid and dashed vertical lines at ipsilateral foot-strike and contralateral foot-off, respectively. Standard deviation band of simulated (OpenSim) and experimental plug-in gait (Vicon PiG) kinematics shown. Only sagittal plane ankle and knee data presented as musculo-skeletal model subtalar joint was locked for simulation and knee has a single flexion/extension axis, respectively. Full gait cycle created by merging data from both limbs.

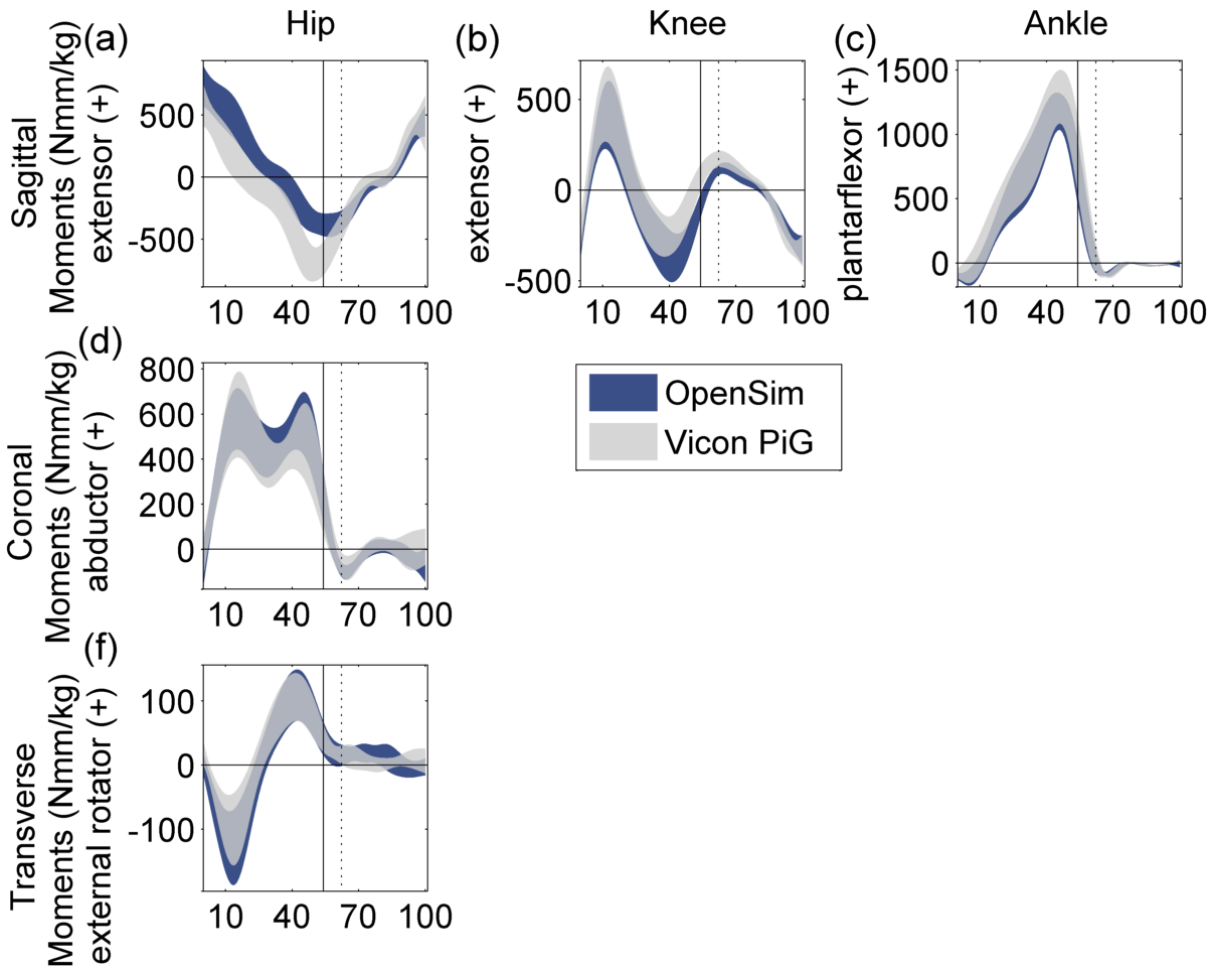

Supplemental Fig. 2: Hip, knee, and ankle joint moments during straight walking (x–axis: 0–100% of the gait cycle) with solid and dashed vertical lines at ipsilateral foot-strike and contralateral foot-off, respectively. Standard deviation band of simulated (OpenSim) and experimental plug-in gait (Vicon PiG) kinetics shown. Only sagittal plane ankle and knee data presented as musculo-skeletal model subtalar joint was locked for simulation and knee has a single flexion/extension axis, respectively. Full gait cycle created by merging data from both limbs.

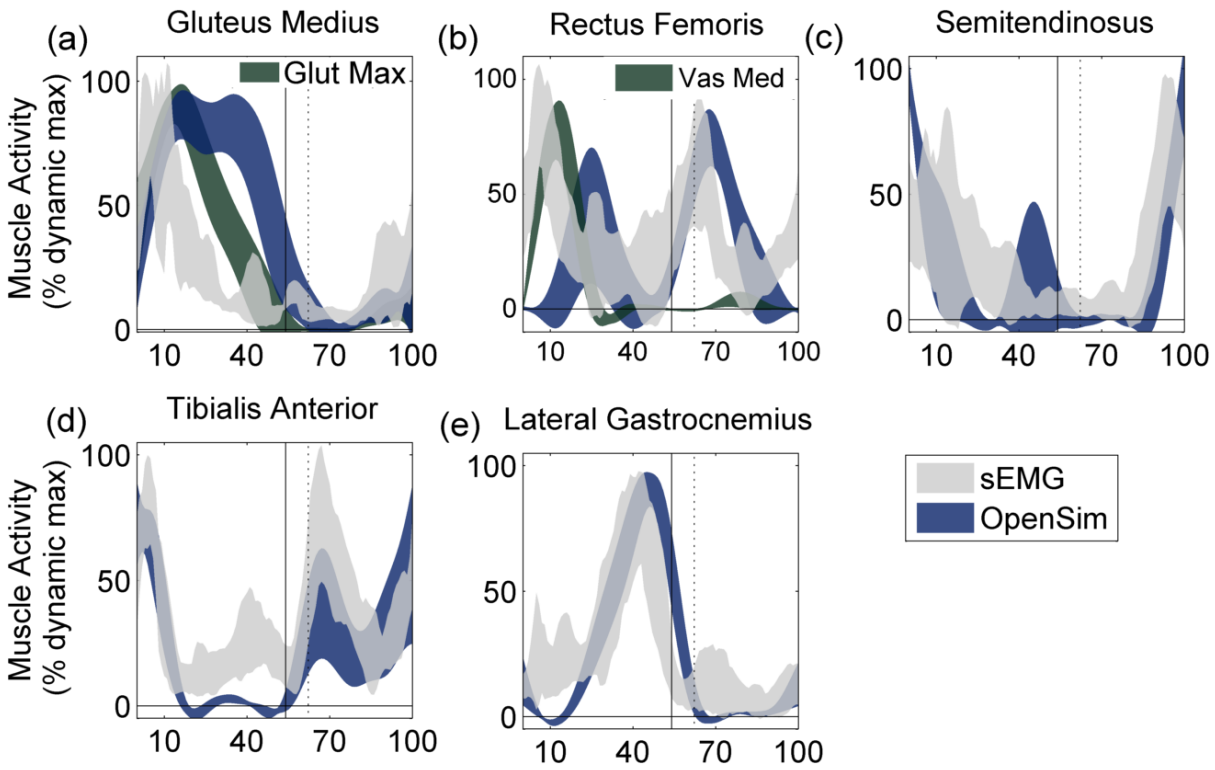

Supplemental Fig. 3: Muscle activity during straight walking (x–axis: 0–100% of the gait cycle) with solid and dashed vertical lines at ipsilateral foot-strike and contralateral foot-off, respectively. Standard deviation band of simulated (OpenSim) and processed surface electromyographic (sEMG) data presented for (a) Gluteus Medius, (b) Rectus Femoris, (c) Semitendinosus, (d) Tibialis Anterior, and (e) Lateral Gastrocnemius. For (a) and (b) Gluteus Medius (Glut Med) and Vastus Medialis (Vas Med) activity from OpenSim, respectively, also shown. Full gait cycle created by merging data from both limbs. Glut Med activity recorded for n = 4 subjects.

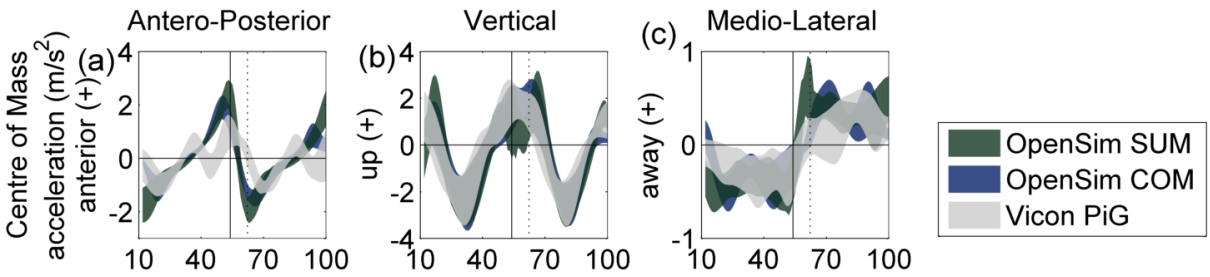

Supplemental Fig. 4: Centre of mass (COM) acceleration in the (a) antero-posterior, (b) vertical, and (c) medio-lateral direction during straight walking (x–axis: 12–100% of the gait cycle) with solid and dashed vertical lines at ipsilateral foot-strike and contralateral foot-off, respectively. Standard deviation band of sum of all muscle accelerations (OpenSim Sum), second derivative of COM position from simulations (OpenSim COM), and second derivative of plug-in gait model COM position (Vicon PiG) shown.

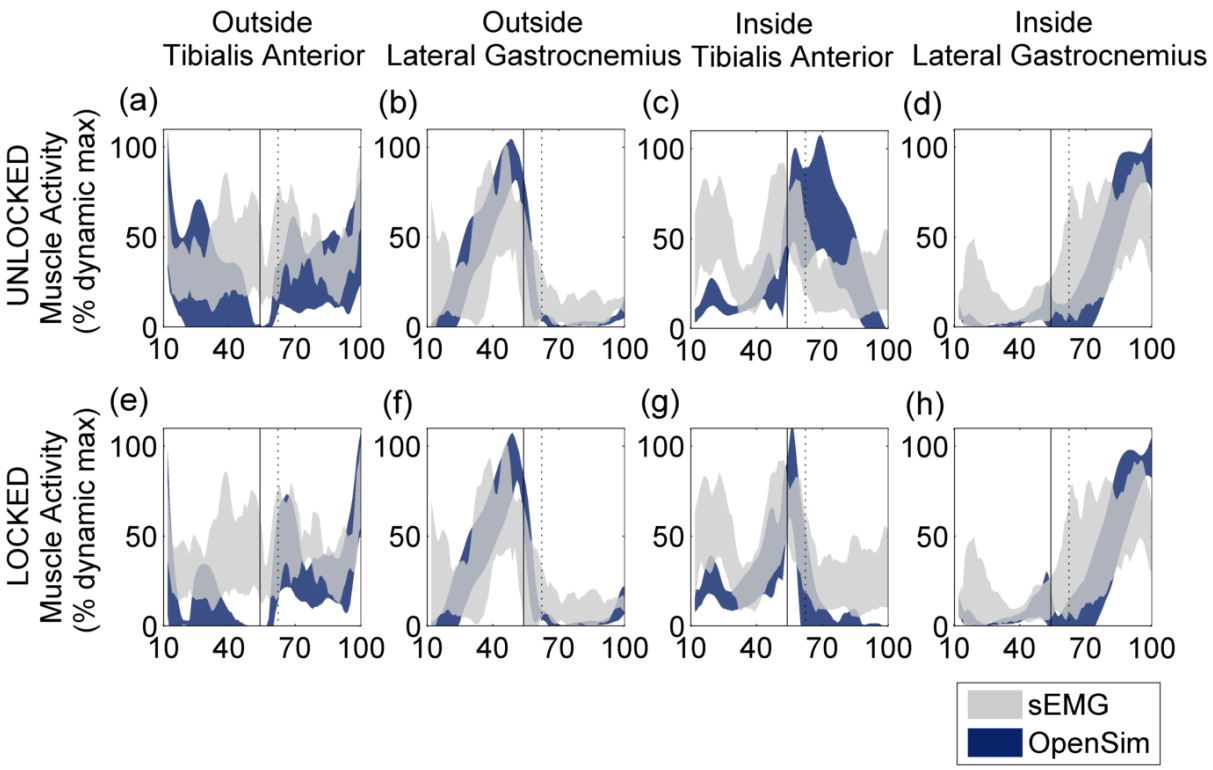

Supplemental Fig. 5: Muscle activity during spin turns (x–axis: 12–100% of the gait cycle) with solid and dashed vertical lines at inside foot-strike and outside foot-off, respectively. Standard deviation band of simulated (OpenSim) and processed surface electromyographic (sEMG) data presented for outside Tibialis Anterior (a and e), outside Lateral Gastrocnemius (b and f), inside Tibialis Anterior (c and g), and inside Lateral Gastrocnemius (d and h). Top and bottom row show effect of unlocking and locking the subtalar joint, respectively, on simulated muscle activity.

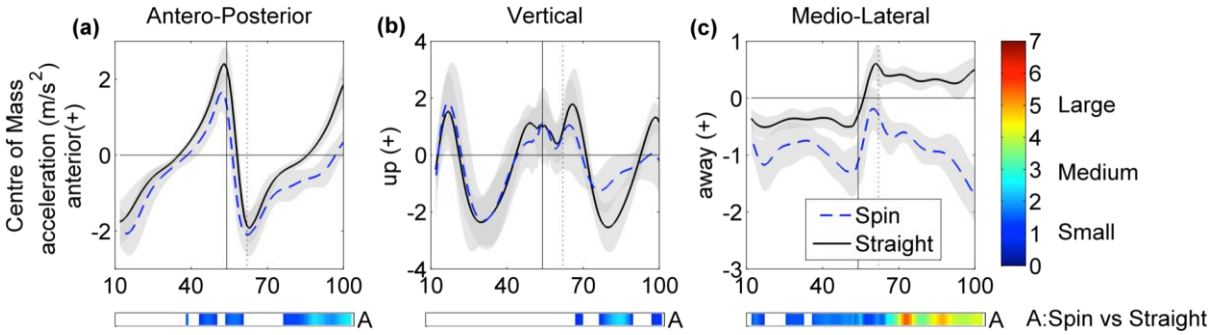

Supplemental Fig. 6: Centre of mass acceleration in the (a) antero-posterior, (b) vertical, and (c) medio-lateral direction during straight and spin turn conditions (x–axis: 12–100% of the gait cycle) with solid and dashed vertical lines at inside foot-strike and outside foot-off, respectively. Variability constructed from Bootstrap confidence bands (CB). Colorbars show areas where mean difference CBs revealed significant differences at $\alpha = 0.05$ with intensity representing effect size of the differences varying from small (blue) to large (red). Zones of significant difference with changes of less than 5% of maximum CB width not shown. See (Dixon et al., 2013) for details of Bootstrap statistical analysis methodology.